1   **Microplastic and microfiber fluxes in the Seine River: Flood events versus Dry periods**

2

3   TREILLES Robin[1*], GASPERI Johnny[2], TRAMOY Romain[1], DRIS Rachid[1], GALLARD

4   Anaïs[1], PARTIBANE Chandirane[1], TASSIN Bruno[1]

5

6   [1] Leesu, Ecole des Ponts, Univ Paris Est Creteil, Marne-la-Vallee, France

7

8   [2] GERS-LEE Université Gustave Eiffel, IFSTTAR, F-44344 Bouguenais, France

9   *Corresponding author: robin.treilles@enpc.fr

10

11   Abstract

12   Studies on the influence of hydrodynamic conditions on anthropogenic microfiber (MF) and

13   microplastic (MP) distributions in freshwater environments are sparse. In this study, we

14   studied the influence of urbanisation gradient on the spatial variability of MFs and MPs.

15   Temporal variability was also assessed by comparing the concentrations and fluxes of MFs

16   and MPs under low flow conditions with those during the January-February 2018 flood event.

17   For each period, Seine river water was collected upstream and downstream of Greater Paris

18   and filtered through an 80 µm net at three different sampling sites. MFs were counted using

19   a stereomicroscope, while MPs were analysed using micro-Fourier transform infrared

20   spectroscopy coupled with siMPle analysis software. The highest concentrations of MFs and

21   MPs were reported at the furthest downstream sites during both periods. However, high

22   water flowrates and urbanisation gradient did not significantly impact MF and MP

23   concentrations, sizes, or polymer distributions. The median MF and MP concentrations were

24   2.6 and 15.5 items/L and their interquartile ranges were 1.6 and 4.9 items/L (n=10),

25   respectively, illustrating relatively stable concentrations in spite of the urbanisation gradient

26   and variations in the flowrate. In contrast to the concentration, size, and polymer distribution

27   characteristics, MP mass fluxes were strongly affected by river flow. MF and MP fluxes show

28   increases in the number and mass of particles from upstream to downstream. The

29   downstream site presents high MP mass fluxes, which range between 924 and 1675

30   tonnes/year. These results may indicate significant MP inputs from the Paris Megacity

31   through wastewater treatment plant effluents and untreated stormwater. The January-

32   February 2018 flood event, which represented 14.5% of the year (in terms of time),

33   contributed 40% of the yearly MP mass fluxes. Thus, flood events contribute strongly to MP

34   fluxes.

35   KEYWORDS: microplastic, microfiber, microlitter, plastic pollution, flood, hydrological

36   conditions

37   Graphical abstract

38
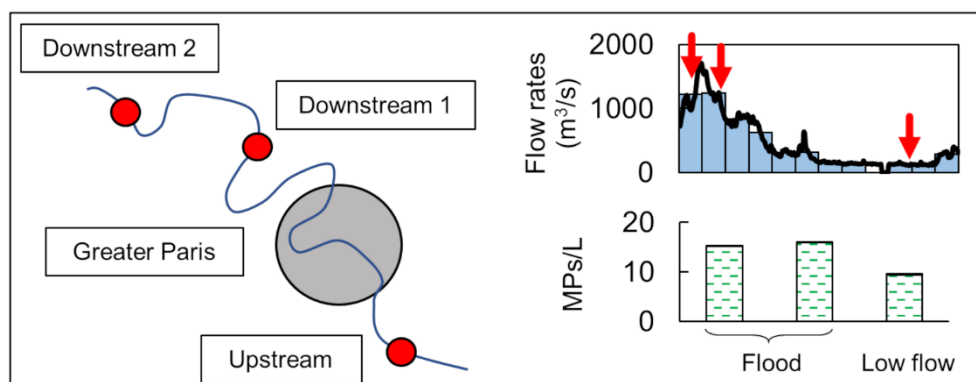
39   1.   Introduction

40   Microlitter, such as microfibers (MFs) and microplastics (MPs), represent a threat to marine

41   (Cole et al., 2011; Gall and Thompson, 2015; Jamieson A. J. et al., 2019) and freshwater

42   environments (Blettler et al., 2017). An increasing number of studies have investigated the

43   transport of microlitter in freshwater environments. The development of microlitter analysis in

44   environmental matrices such as surface waters (Horton et al., 2017) and sediments (Klein et

45   al., 2015) has led to significant advances in assessing the concentration of these particles.

46 However, very few studies have been conducted on the influence of hydrological conditions

47 and urbanisation gradients on microlitter concentrations in rivers.

48 Several studies have observed higher concentrations of microlitter during low-flow periods

49 than in high-flow conditions (de Carvalho et al., 2021; Rodrigues et al., 2018; Watkins et al.,

50 2019; Wu et al., 2020). This difference in concentrations was attributed to a dilution effect.

51 Other studies did not observe significant differences in microlitter concentrations between

52 low and high-flow conditions (Schmidt et al., 2018; Wagner et al., 2019). According to these

53 studies, other parameters may influence the microlitter concentrations. Several studies did

54 not evaluate variation linked to flowrate seasonality, but focused on the impact of rain events

55 during low-flow conditions. Hitchcock (2020) showed that under low-flow conditions, the MP

56 concentration of a small urban estuary river increased during two days of heavy rain, from

57 400 particles/m^3 to 17 000 particles/m^3. Wong et al. (2020) observed a correlation between

58 MP concentrations and precipitation in freshwater environments and noted a strong impact

59 of runoff on MP distribution. Rain events may increase the MP input in rivers owing to the

60 leaching of soil and sealed surfaces. Rain events can lead to combined sewer overflows and

61 untreated stormwater discharge to rivers (Blettler et al., 2017). Thus, rain events may induce

62 a flushing effect, that is, an increase in the MP input to freshwater resulting from

63 mismanaged urban water (Schmidt et al., 2018). Other studies have suggested that there is

64 no simple correlation between river flow and MP concentration (Kataoka et al., 2019;

65 Wagner et al., 2019). Kataoka et al. (2019) observed a correlation between MP

66 concentrations and water quality, but no relationship between MP concentrations and

67 flowrates. Other studies have shown that flood events may play a key role in plastic debris

68 loads in rivers (Roebroek et al., 2021; Tramoy et al., 2020b). Veerasingam et al. (2016)

69 observed a significant increase in MP pellet concentrations in beach sediments after a flood

70 event. These pellets may have been remobilised and more easily migrated from land to sea.

71 Hurley et al. (2018) showed that a significant amount of the MP load stored in channel-bed

72 sediments was exported after a flood. According to these studies, MPs may be efficiently

73 flushed from the river to the sea during a flood. Anthropogenic MFs are rarely considered in

74 these studies, even though they are ubiquitous contaminants (Zhao et al., 2016). Thus, the

75 relationship between microlitter concentration, flow rates, and precipitation is still debated.

76 Several studies concerning the influence of the urbanisation gradient have observed higher

77 MP concentrations in urbanised, densely populated, and downstream areas (Kataoka et al.,

78 2019; Schmidt et al., 2018; Wagner et al., 2019; Wu et al., 2020). In several of these studies,

79 MP concentrations were correlated with population density (Kataoka et al., 2019; Wu et al.,

80 2020). According to Wagner et al. (2019), plastic concentrations may be constant in rural

81 areas but increase linearly in urban areas owing to inputs associated with urban discharge

82 during rainy weather. Rodrigues et al. (2018) observed higher concentrations upstream of

83 the catchment studied. This observation may be a particular to the sampling site, as the

84 upstream part of the catchment studied has a higher population density (Rodrigues et al.,

85 2018). However, Wong et al. (2020) observed no correlation between MP concentrations

86 and population density. Thus, various conclusions may be drawn, depending on the

87 sampling site.

88 In this study, MF and MP concentrations were estimated at three different sampling sites

89 upstream and downstream from Greater Paris during low flow conditions, as well as during a

90 flood event that occurred in January-February 2018. The main objectives of this work were

91 to evaluate the influence of the urbanisation gradient and different hydrological conditions on

92 the MF and MP concentrations and fluxes.

93 2. Materials and methods

94   2.1. Sampling sites

95 Three sampling sites were selected: (i) the first site, noted "Upstream", is located 100 km

96 upstream of Paris (Greater Paris, 8.9 million capita, 2 546 km^2, 3 700 cap/km^2) and

97 downstream of the moderately dense city of Troyes (Troyes Champagne Metropolis,

98 170 167 capita, 889 km^2, 191 cap/km^2, with a waste water treatment plant capacity of 260

99   000 population equivalent) ; (ii) the two other sites are located 20 and 45 km downstream of

100   Paris and noted as "Downstream 1" and "Downstream 2", respectively. Upstream is less

101   impacted by industrial activities, whereas Downstream 1 and 2 correspond to a dense

102   urbanised area. Downstream 1 is located downstream from three significant waste water

103   treatment plants (noted as WWTP, "Seine Centre", "Seine Amont" and "Marne Aval", which

104   have treatment capacities of 240 000, 600 000 and 75 000 m^3 per day, respectively),

105   Downstream 2 is located downstream of the most significant WWTP of Paris Megacity

106   (Seine Aval, which has a treatment capacity of 1 700 000 m^3 per day, according to the

107   Parisian Public Sanitation Authority) and is also located downstream of the confluence

108   between the Seine River and Oise River, which is one of its main tributaries (Figure 1). The

109   major potential sources of microplastics are: (i) Combined Sewer Overflows (CSO) of

110   Greater Paris, (ii) Waste Water Treatment Plants (treatment capacity > 75 000 m^3 per day),

111   (iii) untreated stormwater, and (iv) densely populated areas with intense industrial activities

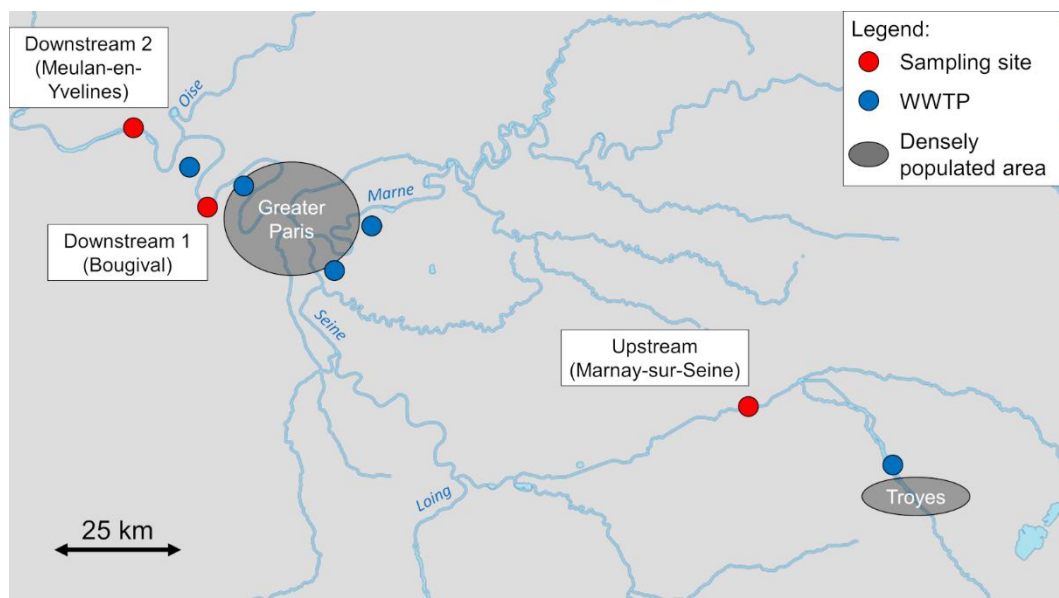112   near the different sampling sites.

113

114   Figure 1: Location of the sampling sites, most significant Wastewater Treatment Plants

115   (WWTPs, treatment capacity > 75 000 m^3 per day) and densely populated areas (the

116   hydrographic network is from Geoportail France).

5

117   2.2. Sampling method

118   Three sampling campaigns were performed during contrasting hydrological conditions: two

119   campaigns were conducted during the flood event that occurred in January-February 2018,

120   represented by the numbers 1 and 2 in Figure 2 (01/26/18 and 02/21/18, $Q_{max\ Paris}$ = 1710

121   m^3/s, with a 10 year return period of Q_{10} = 1650 m^3/s and a 100 year return period of Q_{100} =

122   2400 m^3/s) and one campaign was conducted during the dry season during a low water level

123   period, represented by the number 3 in Figure 2 (07/17/18, Q_{Paris} = 155 m^3/s). The Seine

124   River was monitored by a surveillance network that followed the flow variations (Figure 2).

125   Samples were collected at each site during the same day in the following order: Upstream,

126   Downstream 1, and Downstream 2. One extra sample was collected on 02/21/18 from the

127   Upstream sampling site (2 bis, green arrow in Figure 2). The first campaign (01/26/18)

128   corresponded to a period of increasing flow just before the flow peak. The following

129   campaign in February 2018 corresponded to a decrease in the water flowrate. The daily

130   flowrates and water levels of each sampling campaign are presented in the supplementary

131   data (Table S1). Between 20 and 30 L of water were manually collected from the bridges

132   using a metal bucket and filtered through an 80 µm net. Plastic materials were banned to

133   avoid any on-site contamination. The net was systematically rinsed before and after

134   sampling. The samples were then stored in glass containers in a cold room (4°C).
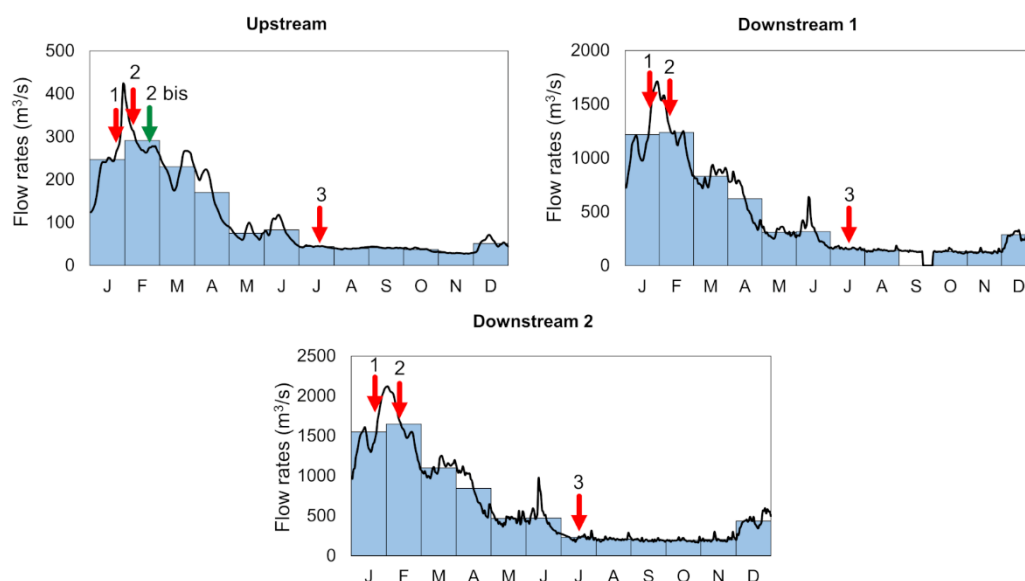
Figure 2: Daily flowrates (black lines) and monthly mean flowrate (blue bars) of the different sampling sites for 2018. Date of sampling is represented by the red arrows (data from http://hydro.eaufrance.fr, Upstream, Downstream 1 and Downstream 2 flowrates were assessed using Pont-sur-Seine, Austerlitz and Vernon measurements, respectively). The green arrow indicate the extra sample collected at the Upstream sampling site.

2.3. Analytical procedure

Samples were sieved using a 5 mm and a 1 mm sieve and separated into the 1-5 mm fraction and <1 mm fraction. Sieving did not prevent the entrance of long fibers (> 5 mm) in the <1 mm fraction, owing to their small diametres. Particles in the 1-5 mm fractions were inspected under a stereomicroscope. Based on their colour, shape, and texture, suspected plastic particles were set aside and characterised using infrared spectroscopy with attenuated total reflectance (ATR-FTIR, Thermo Scientific™ iD7 accessory). This method is based on Dris et al., 2017. For the <1 mm fraction, organic matter was oxidised using 30 wt% H_2O_2 digestion at 40°C for 48 h with 50 mL of solution and magnetic stirring (300 rpm). Digestion was conducted at temperatures ≤ 40°C to avoid thermal degradation of the MFs (Treilles et al., 2020). The solution was filtered through a metallic filter (Ø = 90 mm, porosity = 14 μm). MP particles were then separated from mineral matter by densimetric separation

153   in a NaI solution ($\rho \geq 1.6$ g.cm^{-3}) in a separating funnel. The supernatant was filtered using

154   the same metallic filters and the microlitter was characterised.

155   Because of their shapes, the automatization of MF detection with µFTIR and processing

156   software cannot be implemented confidently. Indeed, confusions between MFs and MP

157   fragments were frequently observed with automated µFTIR detection. For this reason, all

158   MFs were manually counted under a stereomicroscope (Leica MZ12, with a size detection

159   limit of 50 µm) coupled with an image analysis software (Histolab) according to the method

160   developed by Dris et al. (2018), while MPs were counted and chemically characterized by

161   µFTIR imaging, with no shape distinction. MFs are all anthropogenic fibers, including

162   synthetic and non-synthetic fibers. This results in possible crossed data between MFs and

163   MPs. However, we decided to keep the data in this form, as the size distribution between

164   MPs and MFs is significantly different (Figure 5). Indeed, most of MPs are below 250 µm

165   whereas MFs are above 1000 µm (Figure 5). This overlap of data may thus be negligible.

166   Once the MFs were counted, metallic filters were plunged in a crystallizer with 20 mL of

167   filtered water and the particles were removed using an ultrasonic bath for 30 s. The filtered

168   water was then poured into a 100 mL glass bottle. This resuspension step was repeated

169   three times. Then, the metallic filter was rinsed one last time with 40 mL of filtered water.

170   The glass bottle was vigorously stirred for 1 min to homogenise the content. Then, 10 to 20

171   mL of this volume, *i.e.,* 10 to 20 %, was filtered onto a Whatman® anodisc inorganic filter

172   membrane (porosity: 0.2 µm, Ø 25 mm, with a filtration surface of Ø 14 mm).

173   The anodisc filters were analysed with Fourier transform infrared spectroscopy coupled with

174   a microscope, using the Thermo Scientific Nicolet™ iN10 µFTIR in transmission mode. A

175   Thermo Scientific® MCT/A Cooled Imaging detector with a spectral range of 4000 to

176   1200 cm^{-1} was used to avoid interference with the anodisc filter. An autobaseline correction

177   was applied to all spectra. After the spectral background was defined, the mapping analysis

178   mode was used on one scan. All particles on three 6 × 6 mm infrared maps were analysed,

179   corresponding to 70% of the filtration surface of the filter. An atmospheric suppression

180   correction was applied to all spectra. Maps were analysed using the siMPle analysis

181 software developed by Aalborg University, Denmark and the Alfred Wegener Institute,

182 Germany (Liu et al., 2019).

183 This method has a size detection limit of 25 µm. Each spectrum identified as a plastic

184 polymer by the siMPle software was checked by an operator for false positives. Particular

185 attention was paid to PE spectra, as false positives of these particles have been observed in

186 other studies (Witzig et al., 2020). siMPle assesses the number of particles and estimates an

187 order of magnitude for the mass and volume of MPs, as detailed in Kirstein et al., 2021. MP

188 concentrations were extrapolated to the initial sampling volumes. Because the number of

189 samples remained small, non-parametric statistics were used in the analysis.

190 Several precautions were applied to mitigate contamination. Glass vessels and filters were

191 all heated to 500°C for 2 h before use. All solutions used were filtered on GF/D Whatman

192 glass fibre filters (Sigma Aldrich, porosity: 2.7 µm). The vessels were rinsed with filtered

193 water and filtered using 50% ethanol. Laboratory coats of 100% cotton were worn and

194 plastic materials were avoided. The samples were stored in glass bottles. Glass bottles and

195 all beakers were covered with aluminium foil. The samples were sieved using a laminar flow

196 cabinet. Contamination during the different extraction steps was evaluated using procedural

197 blanks (n=10), which underwent the same steps as the samples.

198 3. Results and discussion

199   3.1. Microfiber and microplastic concentrations

200 During the flood event, MF concentrations ranged between 1.3 and 3.7 items/L, whereas MP

201 concentrations ranged from 10.4 to 34.4 items/L (Figure 3). In low flow conditions, MF

202 concentrations ranged from 1.9 to 5.5 items/L, whereas MP concentrations ranged from 9.3

203 to 26.5 items/L (min–max values). Median MF contamination was 0.3 items/L with an

204 interquartile range of 0.2 (n=10) whereas median MP contamination was 0.2 items/L with an

205 interquartile range of 0.2 (Figure 3).

206 Variations in the minimum and maximum concentrations of all samples were calculated for

207 each sampling site, under low flow conditions and during the flood (variation in concentration

208 = (Max-Min)/Min) * 100) (Table 1). Upstream and Downstream 1 presented relatively low

209 variations between the minimum and maximum concentrations for both MFs (< 25%) and

210 MPs (<71%) (Table 1). Downstream 2 presented the highest MF (229.8%) and MP

211 concentrations (318.0%) (Figure 3) and the highest variability between minimum and

212 maximum values (Table 1).

213 Table 1: Variation in concentrations between minimum and maximum values for each

214 sampling site, for samples collected in low flow conditions and during the flood

	%Variation between min-max values for **MFs**	%Variation between min-max values for **MPs**
Upstream	14.4	49.0
Downstream 1	23.3	70.3
Downstream 2	318.0	229.8

215

216 If all samples are combined, we obtain MF and MP median concentrations of 2.6 and 15.5

217 items/L and interquartile ranges of 1.6 and 4.9 items/L, respectively (n = 10). Other studies

218 in freshwater environments generally have found concentrations below 1 items/L (de

219 Carvalho et al., 2021; Kataoka et al., 2019; Wong et al., 2020). The concentrations we found

220 are comparable to those found in Cooks River, Australia (between 0.4 and 17.4 items/L,

221 Hitchcock, 2020) and in the Maozhou River, China (between 3.5 and 25.5 items/L, Wu et al.,

222 2020). We found that MPs were more abundant than MFs. Several studies have also

223 reported fewer fibers than other shapes in freshwater samples (Mani and Burkhardt-Holm,

224 2020; Mao et al., 2020; Wu et al., 2020). Stereomicroscope counting did not enable the

225 detection of MFs below 50 µm. Therefore, we may have underestimated the MF

226 concentration. Despite a strong urban gradient and high water flow variability between

227 sampling sites, MF and MP concentrations during low flow conditions have the same order

228 of magnitude as the concentrations estimated during the flood event of January-February

229   2018 (Figure 3 and Table 1). Downstream 2 presented the highest variability (Table 1) and

230   the highest concentrations (Figure 3) of MPs and MFs, both during low-flow conditions and

231   the flood event. This may indicate a significant release of MPs related to WWTPs. However,

232   Downstream 2 is located downstream the confluence with the Oise River (Figure 1), which

233   was also flooded. This tributary is less urbanised and may dilute the microlitter inputs at this

234   sampling site. However, the flood event did not significantly change the concentrations

235   observed at the different sampling sites. As previously noted, contradictory results were

236   found regarding the influence of water levels and flows on MP concentrations. The dilution of

237   MPs during flood events has been reported in several studies (Rodrigues et al., 2018;

238   Watkins et al., 2019; Wu et al., 2020), but does not seem to occur in the Seine River. Recent

239   studies have shown that stormwater runoff could be a significant source of macroplastics

240   (Treilles et al., 2021b) and microplastics during rain events (C. Liu et al., 2019; Treilles et al.,

241   2021a). Precipitation may increase microlitter inputs through stormwater runoff. The increase

242   in the flowrate during a flood implies remobilisation of the sediments owing to an increase in

243   the shear strength, as well as remobilisation of MF and MP stored in sediments (Hurley et

244   al., 2018). However, in the Seine River, waterway traffic may greatly influence this

245   distribution. In 2019, 23.7 millions of tons of goods were transported by waterway traffic in

246   the Seine River basin (Voies Navigables de France, 2020). This intense activity influences

247   the sediment dynamics, which are not in a steady state (Vilmin, 2014). Waterway traffic

248   intensively remobilises sediments even under low-flow conditions. This could partially

249   explain the similar values observed between the flood and low-flow conditions. To ensure

250   better comparability between studies, waterway traffic and sediment dynamics in a study

251   area should be precisely recorded. The concentrations found in the Seine River are very

252   high compared to those presented in a previous study on this river ($\sim 3 \times 10^{-4}$ MPs/L ; Dris et

253   al., 2015). The Seine River concentrations are also high compared to those found in the

254   Rhine ($\sim 1 \times 10$–3MPs/L ; Mani et al., 2015). Contrary to Wong et al. (2020), we found no

255   statistically significant correlations between precipitation and concentration (Spearman's rs
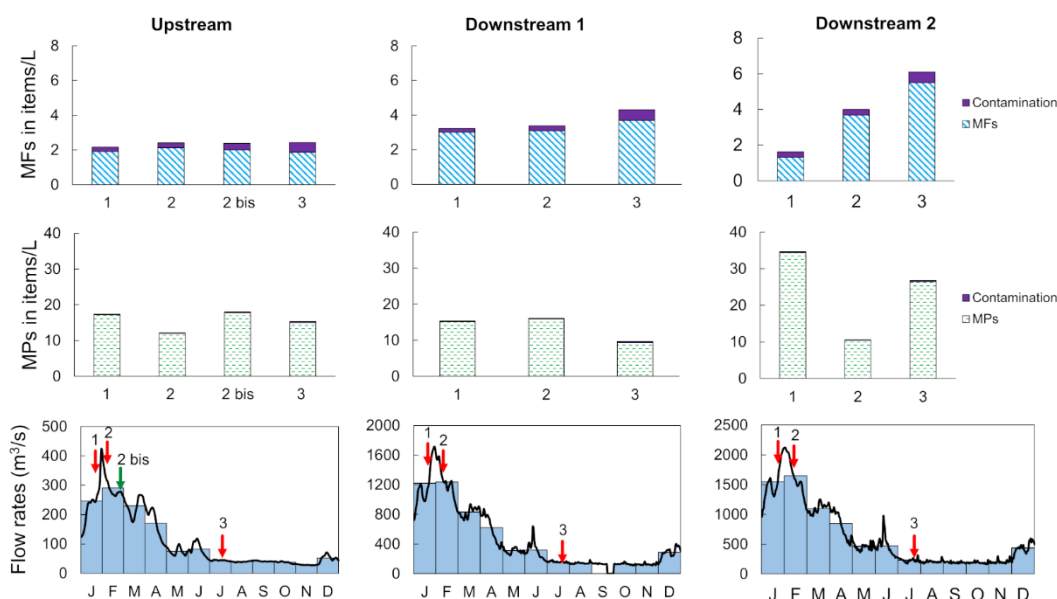
256   test, $p = 0.89$).

Figure 3: Microfiber and microplastic concentrations in the Seine river, relative to the

hydrograph of each site (y-axis are different depending on the sampling site)

Regarding the spatial variations, concentrations between the upstream and downstream

areas were of the same order of magnitude. This is consistent with previous data collected

by Dris et al. (2018), who did not notice a significant impact of the urban gradient or

variations in the flow rate on the MF or MP concentrations in the Seine River. These

observations were confirmed by the present study at a larger scale. Based on the size and

shape of the particles, the siMPle analysis software enables MP mass concentration

estimates. However, it was not possible to estimate the mass of the MFs that we counted

using a stereomicroscope. The order of magnitude for MP mass concentrations was

comparable between the low flow period and the flood event, as shown in Table 2. We did

not observe a significant concentration gradient between the upstream and downstream

sites of Greater Paris in terms of mass concentrations, which is consistent with the results of

Dris et al. (2018). In addition, Downstream 2 presented the highest mass concentrations in

number of particles (Table 2). MP mass concentrations in freshwater environments have

been only rarely estimated. Using the total weight/number of microplastics and non-metric

multidimensional scaling (nMDS), Rodrigues et al., 2018 reported mass concentrations

between 5 and 51.7 µg/L in Antuã River, Portugal. These values were comparable to our

12

276   estimations. Several studies have reported lower mass concentrations. In surface water

277   samples, Haberstroh et al. (2021) found a mean mass concentration of 5.4 µg/L in the

278   Hillsborough River, USA. Kataoka et al. (2019) observed variable MP mass concentrations

279   between 0 and 3.2 µg/L.

280   Table 2: Estimation of MP mass concentrations in Seine River water based on siMPle

281   software analysis.

	Median mass concentration during low flow period (µg/L)	Median mass concentration during the flood event (µg/L)
Upstream	10	20
Downstream 1	5	10
Downstream 2	80	50

282

283   3.2. Microfiber and microplastic size distribution

284   Boxplots of the MF and MP sizes relative to river discharge are shown in Figure 4. The size

285   distribution of these particles under low-flow conditions and during the flood event is

286   presented in Figure 5. During the flood event, the median MF sizes of Upstream,

287   Downstream 1, and Downstream 2 samples ranged from 1960 to 5410 µm, whereas the

288   median MP sizes ranged from 115 to 205 µm (Figure 4). The MF size distribution showed

289   the presence of large MFs >5 mm (Figure 5).

290   In low-flow conditions, the median MF sizes of Upstream, Downstream 1, and Downstream 2

291   samples ranged from 2500 to 3480 µm, whereas the median MP size ranged from 96 to 248

292   µm (Figure 4). As for the flood event, the MF size distribution showed the presence of large

293   MFs >5 mm (Figure 5). In contrast, the median MP size was below 250 µm. The MF and MP

294   size distributions during the flood and low-flow conditions are detailed in the supplementary

295   data (Table S2 and Table S3). The mean values were always higher than the median values

296   owing to the presence of large particles (> 5 mm for MFs and > 1 mm for MPs) (Figure 4).
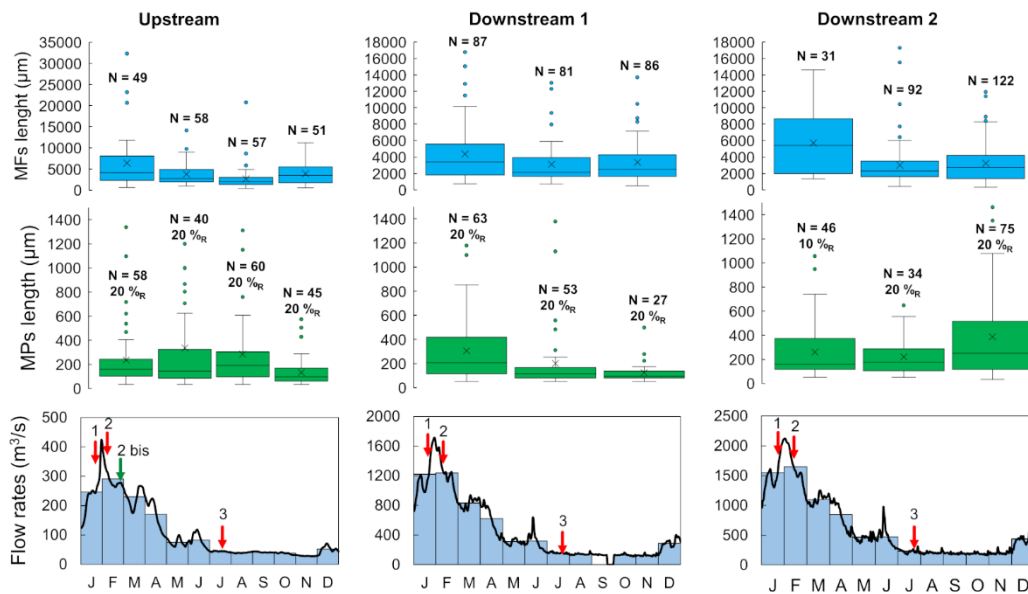
297

Figure 4: Boxplots of microfiber and microplastic length relative to the hydrographs of each

sampling site (y-axis may be different depending on the sampling site); mean values are

displayed as crosses; $\%_R$: resuspension percentage; N: number of particles
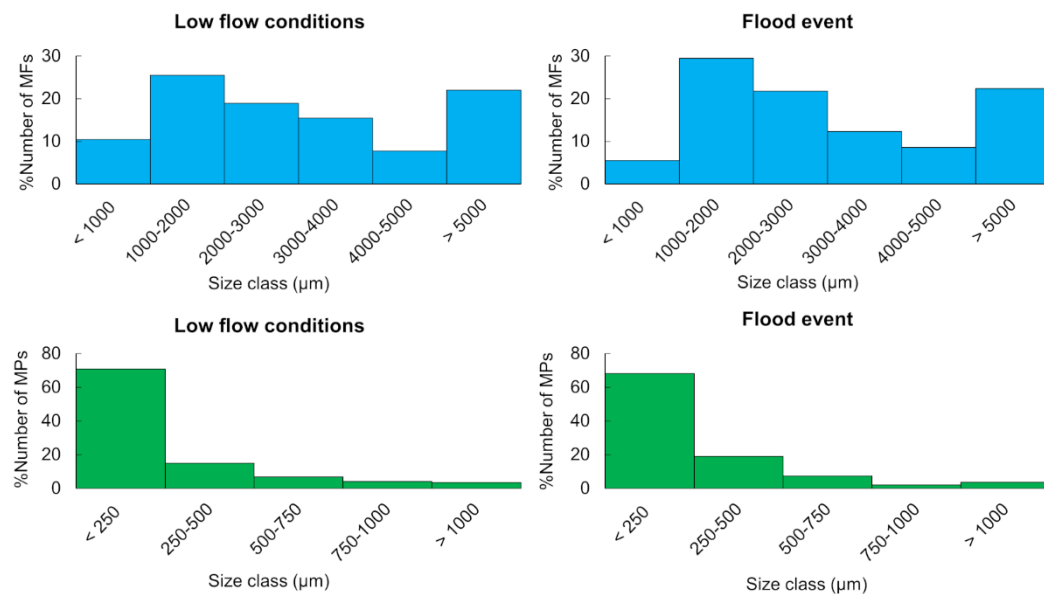

301

Figure 5: Microfiber and microplastic size distributions in low flow conditions and during the

flood event

According to Figure 5, the size distributions in low-flow conditions and during the flood event

are similar. MFs sizes were not significantly different between times of low river discharge

and floods, according to the Mann-Whitney test (n=259 in low flow conditions and n=455

14

307 during the flood; p = 0.33). The same trend was observed for MPs (MW test, n=147 in low-

308 flow conditions and n=354 during the flood; p = 0.09). MFs and MPs found in the analytical

309 blanks were significantly smaller than the particles analysed in the samples (MW test, p

310 <0.05). The median number of MF and MP found in each analytical blank was 9 and 4,

311 respectively, with a median size of 1800 µm and 104 µm, respectively (n=10).

312 More than 20% of MFs belonged to the > 5 mm size class (Figure 5). The minimum and

313 maximum MF sizes of all the samples were 313 and 32328 µm, respectively. Even though

314 more than 60% of MFs are smaller than 4 mm, the <1 mm size class is not the most

315 abundant, in contrast with the size distribution of MFs found in atmospheric fallout (Allen et

316 al., 2019). This size distribution differs from that found in a previous study on the Seine

317 River, for which >1 mm was the most significant fraction (Dris et al., 2018).

318 More than 60% of MPs were smaller than 250 µm (Figure 5). This shows the importance of

319 using a small mesh size for MP sampling. A 300 µm net may be inefficient in collecting the

320 most significant MP size classes. The minimum and maximum MP sizes of all samples

321 combined were 32 µm and 2 528 µm, respectively. When all samples were combined (for

322 low flow periods and during the flood), 20% of all MPs were smaller than 80 µm. This may

323 indicate that: (i) the 80 µm net clogged and stored small MPs or (ii) MP aggregates with

324 various MP sizes could have accumulated in the net and could have been separated during

325 organic matter digestion.

326   3.3. Polymer distribution

327 Polypropylene (PP) is the most common polymer (56–90%), followed by polyethylene (PE,

328 3–19%) and polyester (PES, 0–26%) in all samples (Figure 6). The category "other" from

329 Figure 6 contains seven polymers, as detailed in the supplementary data (Table S4). For all

330 samples, PP was always the most abundant polymer. PP and PE are commonly used in

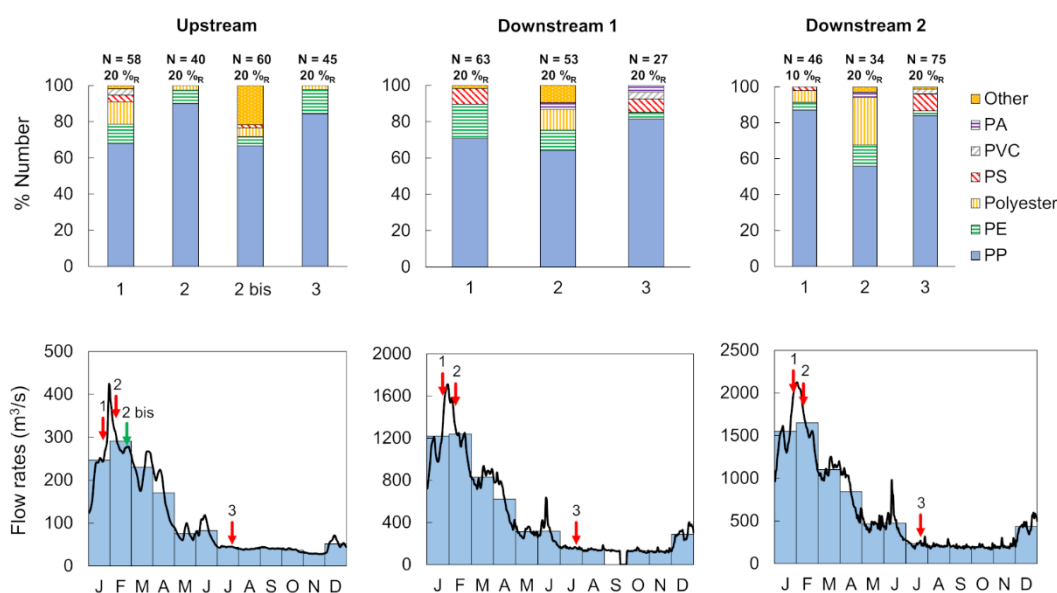331 packaging, while PES is used in plastic bottles and textiles.

Figure 6: Percentage of polymers in each sample relative to river discharge at each site. N: number of microplastics (MP) particles found for a given resuspension volume; $\%_R$: resuspension percentage. PP: polypropylene; PE: polyethylene; PS: polystyrene; PVC: polyvinyl chloride; PA: polyamide;

The results do not show significant differences in polymer distributions between low flow conditions and the flood event (Figure 4-6, Table S4). The most significant polymers found in our samples (PP, PE, PES) are the same as the most representative polymers of macroplastic debris found in rivers (van Emmerik et al., 2018). These macroplastics may have formed MPs through fragmentation, which could explain the similarity in the polymer nature between these studies. The flood event had no significant impact on the type of polymer transported.

3.4. MPs and MFs fluxes in the Seine river

These similarities between low flow conditions and floods have strong implications for MF and MP fluxes in the Seine River. Considering the daily flowrates of each sampling site (assessed using Pont-sur-Seine, Austerlitz, and Vernon measurements, respectively; see Figure 2) and the MF and MP concentrations (first and third quartiles, see supplementary data Table S6), we calculated the MF and MP fluxes as the number of particles flowing per

350 year in the Seine River. We assumed that the MF and MP distributions were the same over

351 the water column. For both MF and MP fluxes, we observed an increasing gradient from

352 Upstream to Downstream 2 (Table 3).

353 The MF flux ranges from 6.6×10^{12} to 9.1×10^{13} items/year, increasing from Upstream to

354 Downstream 2 (Table 3). Dris et al. (2018) previously estimated an anthropogenic MF flux in

355 the Seine River between 2.8×10^{10} and 6.1×10^{11} particles/year. With the hypothesis that

356 65% of the MFs are synthetic, they approximated a flux between 1.8×10^{10} and 4.0×10^{11} of

357 synthetic MFs per year. Owing to a lack of data, Dris et al. (2018) considered only fibers and

358 not the fragments. We estimated much higher fluxes for anthropogenic MF fluxes. This

359 difference may be linked to methodological differences between our studies. Samples from

360 Dris et al. (2018) were collected with an 80 µm net plunged into the Seine River, while we

361 pre-filtered raw water with an 80 µm net. This sampling difference may affect the

362 concentrations observed in samples, as reported by Zheng et al. (2021), who found a

363 difference in concentration of two orders of magnitude between the pre-filtration method and

364 trawl net for the same sampling site.

365 For MPs, we calculated a flux between 4.9×10^{13} and 6.2×10^{14} items/year, increasing from

366 Upstream to Downstream 2. µFTIR analyses coupled with the analysis software siMPle gave

367 an order of magnitude for MP mass fluxes transported at each sampling site (Table 3). MP

368 mass fluxes ranged between 58 and 1675 tonnes/year and increased from Upstream to

369 Downstream 2. The MP mass fluxes at Downstream 2 are extremely high. The highest MP

370 concentrations (Figure 3, Table 2 and Table S6) and highest flowrates were reported at this

371 site, which explains the reported mass fluxes. As reported for the number of particles,

372 Downstream 2 mass fluxes may be significant due to the different WWTP effluents (Figure

373 1). These significant mass fluxes may indicate high MP loads derived from urban water from

374 the Paris megacity. Thus, MP mass fluxes are impacted by urbanisation.

375   Table 3: Estimations of MF and MP fluxes for each sampling point

	MF Fluxes in items/year	MPs Fluxes in items/year	MPs Fluxes in tonnes/year
Upstream	$6.6\text{-}7.1\times10^{12}$	$4.9\text{-}6.0\times10^{13}$	58-74
Downstream 1	$4.4\text{-}4.8\times10^{13}$	$1.8\text{-}2.2\times10^{14}$	56-146
Downstream 2	$4.9\text{-}9.1\times10^{13}$	$3.6\text{-}6.0\times10^{14}$	924-1675

376

377   The January-February 2018 flood event corresponded to 14.5% of the year (in time) but

378   contributed 40% of the microplastic and microfiber annual loads, indicating the important role

379   of flood events as microplastic inputs in the Seine River. This is consistent with the data

380   collected by Wagner et al. (2019), who found that 90% of the plastic load in freshwater could

381   be transported in 20% of the year. According to our results, we observed a significant

382   increase in MP mass fluxes from upstream to downstream sites, mainly caused by the

383   increase in flow rates and not by a significant concentration increase. For this reason, high

384   water levels may significantly increase the plastic load in freshwater. For macroplastic fluxes,

385   van Emmerik et al. (2019) observed an increase of one order of magnitude during high water

386   levels in the Seine River. According to Tramoy et al. (2020a), flood events may effectively

387   flush plastic debris from upstream to downstream regions owing to their high flow rates.

388   Tramoy et al. (2021, under review) estimated that the macroplastic mass fluxes from the

389   Seine River estuary to the ocean range between 100 and 200 metric tons per year. The high

390   value found in Downstream 2 is most likely linked to the significant mass concentrations and

391   high flowrates for this sampling point. Although MP mass concentrations are rarely assessed

392   in freshwater systems, our results are consistent with the estimations from Rodrigues et al.

393   (2018), but are one or two orders of magnitude higher than other estimations (Haberstroh et

394   al., 2021; Kataoka et al., 2019). These estimations may indicate significant plastic inputs

395   from the Greater Paris region. However, our estimation does not correspond to MP mass

396   discharge from land to sea, but only reflects the MP mass flux at certain sampling points.

397   More data should be collected on plastic mass fluxes, particularly in urban rivers, to confirm

398   the significant microplastic loads we observed.

399   4. Conclusion

400   We evaluated the MF and MP concentrations at three different upstream to downstream

401   sampling sites during both low-flow conditions and a flood event. The results of this study

402   show that the concentrations are of the same order of magnitude regardless of the

403   hydrological conditions. The urbanisation gradient did not significantly influence these

404   concentrations. Similarly, the flood and urbanisation gradient did not significantly affect the

405   size and polymer distributions at the different sampling sites. PP, PE, and PES correspond

406   to more than 60% of all polymers found. However, MP mass fluxes are strongly impacted by

407   the urbanisation gradient, as we observed very high mass fluxes at the most downstream

408   sampling site (924-1675 tonnes/year at Downstream 2). The January-February 2018 flood

409   event, which corresponds to 14.5% of the year (in terms of time), contributed 40% of the MF

410   and MP loads in the Seine River. In the future, greater attention should be paid to flood

411   events, as they constitute major pathways for microlitter contamination. A better

412   understanding of MF and MP dynamics in freshwater environments is needed to evaluate

413   the impact of transitory events such as floods and significant rainfall events.

419   References

420   Allen, S., Allen, D., Phoenix, V.R., Le Roux, G., Durántez Jiménez, P., Simonneau, A., Binet,
421   S., Galop, D., 2019. Atmospheric transport and deposition of microplastics in a
422   remote mountain catchment. Nat. Geosci. 12, 339–344.
423   https://doi.org/10.1038/s41561-019-0335-5
424   Blettler, M.C.M., Ulla, M.A., Rabuffetti, A.P., Garello, N., 2017. Plastic pollution in freshwater
425   ecosystems: macro-, meso-, and microplastic debris in a floodplain lake. Environ.
426   Monit. Assess. 189, 581. https://doi.org/10.1007/s10661-017-6305-8
427   Cole, M., Lindeque, P., Halsband, C., Galloway, T.S., 2011. Microplastics as contaminants in
428   the marine environment: A review. Mar. Pollut. Bull. 62, 2588–2597.
429   https://doi.org/10.1016/j.marpolbul.2011.09.025
430   de Carvalho, A.R., Garcia, F., Riem-Galliano, L., Tudesque, L., Albignac, M., ter Halle, A.,
431   Cucherousset, J., 2021. Urbanization and hydrological conditions drive the spatial
432   and temporal variability of microplastic pollution in the Garonne River. Sci. Total
433   Environ. 769. https://doi.org/10.1016/j.scitotenv.2020.144479
434   Dris, R., Gasperi, J., Mirande, C., Mandin, C., Guerrouache, M., Langlois, V., Tassin, B.,
435   2017. A first overview of textile fibers, including microplastics, in indoor and outdoor
436   environments. Environ. Pollut. 221, 453–458.
437   https://doi.org/10.1016/j.envpol.2016.12.013
438   Dris, R., Gasperi, J., Rocher, V., Saad, M., Renault, N., Tassin, B., 2015. Microplastic
439   contamination in an urban area: a case study in Greater Paris. Environ. Chem. 12,
440   592–599. https://doi.org/10.1071/EN14167
441   Dris, R., Gasperi, J., Tassin, B., 2018. Sources and Fate of Microplastics in Urban Areas: A
442   Focus on Paris Megacity. Freshw. Microplastics 69–83. https://doi.org/10.1007/978-
443   3-319-61615-5_4
444   Gall, S.C., Thompson, R.C., 2015. The impact of debris on marine life. Mar. Pollut. Bull. 92,
445   170–179. https://doi.org/10.1016/j.marpolbul.2014.12.041
446   Haberstroh, C.J., Arias, M.E., Yin, Z., Wang, M.C., 2021. Effects of hydrodynamics on the
447   cross-sectional distribution and transport of plastic in an urban coastal river. Water
448   Environ. Res. 93, 186–200. https://doi.org/10.1002/wer.1386
449   Hitchcock, J.N., 2020. Storm events as key moments of microplastic contamination in
450   aquatic ecosystems. Sci. Total Environ. 734, 139436.
451   https://doi.org/10.1016/j.scitotenv.2020.139436
452   Horton, A.A., Walton, A., Spurgeon, D.J., Lahive, E., Svendsen, C., 2017. Microplastics in
453   freshwater and terrestrial environments: Evaluating the current understanding to
454   identify the knowledge gaps and future research priorities. Sci. Total Environ. 586,
455   127–141. https://doi.org/10.1016/j.scitotenv.2017.01.190
456   Hurley, R., Woodward, J., Rothwell, J., 2018. Microplastic contamination of river beds
457   significantly reduced by catchment-wide flooding. Nat. Geosci.
458   https://doi.org/10.1038/s41561-018-0080-1
459   Jamieson A. J., Brooks L. S. R., Reid W. D. K., Piertney S. B., Narayanaswamy B. E., Linley
460   T. D., 2019. Microplastics and synthetic particles ingested by deep-sea amphipods in
461   six of the deepest marine ecosystems on Earth. R. Soc. Open Sci. 6, 180667.
462   https://doi.org/10.1098/rsos.180667
463   Kataoka, T., Nihei, Y., Kudou, K., Hinata, H., 2019. Assessment of the sources and inflow
464   processes of microplastics in the river environments of Japan. Environ. Pollut. 244,
465   958–965. https://doi.org/10.1016/j.envpol.2018.10.111
466   Kirstein, I.V., Hensel, F., Gomiero, A., Iordachescu, L., Vianello, A., Wittgren, H.B.,
467   Vollertsen, J., 2021. Drinking plastics? – Quantification and qualification of
468   microplastics in drinking water distribution systems by µFTIR and Py-GCMS. Water
469   Res. 188, 116519. https://doi.org/10.1016/j.watres.2020.116519

Klein, S., Worch, E., Knepper, T.P., 2015. Occurrence and Spatial Distribution of
Microplastics in River Shore Sediments of the Rhine-Main Area in Germany. Environ.
Sci. Technol. 49, 6070–6076. https://doi.org/10.1021/acs.est.5b00492

Liu, C., Li, J., Zhang, Y., Wang, L., Deng, J., Gao, Y., Yu, L., Zhang, J., Sun, H., 2019.
Widespread distribution of PET and PC microplastics in dust in urban China and their
estimated human exposure. Environ. Int. 128, 116–124.
https://doi.org/10.1016/j.envint.2019.04.024

Liu, F., Olesen, K.B., Borregaard, A.R., Vollertsen, J., 2019. Microplastics in urban and
highway stormwater retention ponds. Sci. Total Environ. 671, 992–1000.
https://doi.org/10.1016/j.scitotenv.2019.03.416

Mani, T., Burkhardt-Holm, P., 2020. Seasonal microplastics variation in nival and pluvial
stretches of the Rhine River – From the Swiss catchment towards the North Sea. Sci.
Total Environ. 707, 135579. https://doi.org/10.1016/j.scitotenv.2019.135579

Mani, T., Hauk, A., Walter, U., Burkhardt-Holm, P., 2015. Microplastics profile along the
Rhine River. Sci. Rep. 5, 17988. https://doi.org/10.1038/srep17988

Mao, Y., Li, H., Gu, W., Yang, G., Liu, Y., He, Q., 2020. Distribution and characteristics of
microplastics in the Yulin River, China: Role of environmental and spatial factors.
Environ. Pollut. 265, 115033. https://doi.org/10.1016/j.envpol.2020.115033

Rodrigues, M.O., Abrantes, N., Gonçalves, F.J.M., Nogueira, H., Marques, J.C., Gonçalves,
A.M.M., 2018. Spatial and temporal distribution of microplastics in water and
sediments of a freshwater system (Antuã River, Portugal). Sci. Total Environ. 633,
1549–1559. https://doi.org/10.1016/j.scitotenv.2018.03.233

Roebroek, C.T.J., Harrigan, S., Emmerik, T.H.M. van, Baugh, C., Eilander, D., Prudhomme,
C., Pappenberger, F., 2021. Plastic in global rivers: are floods making it worse?
Environ. Res. Lett. 16, 025003. https://doi.org/10.1088/1748-9326/abd5df

Schmidt, L.K., Bochow, M., Imhof, H.K., Oswald, S.E., 2018. Multi-temporal surveys for
microplastic particles enabled by a novel and fast application of SWIR imaging
spectroscopy – Study of an urban watercourse traversing the city of Berlin, Germany.
Environ. Pollut. 239, 579–589. https://doi.org/10.1016/j.envpol.2018.03.097

Tramoy, R., Gasperi, J., Colasse, L., Silvestre, M., Dubois, P., Noûs, C., Tassin, B., 2020a.
Transfer dynamics of macroplastics in estuaries – New insights from the Seine
estuary: Part 2. Short-term dynamics based on GPS-trackers. Mar. Pollut. Bull. 160,
111566. https://doi.org/10.1016/j.marpolbul.2020.111566

Tramoy, R., Gasperi, J., Colasse, L., Tassin, B., 2020b. Transfer dynamic of macroplastics
in estuaries — New insights from the Seine estuary: Part 1. Long term dynamic
based on date-prints on stranded debris. Mar. Pollut. Bull. 152, 110894.
https://doi.org/10.1016/j.marpolbul.2020.110894

Treilles, R., Cayla, A., Gaspéri, J., Strich, B., Ausset, P., Tassin, B., 2020. Impacts of organic
matter digestion protocols on synthetic, artificial and natural raw fibers. Sci. Total
Environ. 748, 141230. https://doi.org/10.1016/j.scitotenv.2020.141230

Treilles, R., Gasperi, J., Gallard, A., Saad, M., Dris, R., Partibane, C., Breton, J., Tassin, B.,
2021a. Microplastics and microfibers in urban runoff from a suburban catchment of
Greater Paris. Sci. Total Environ.

Treilles, R., Gasperi, J., Saad, M., Tramoy, R., Breton, J., Rabier, A., Tassin, B., 2021b.
Abundance, composition and fluxes of plastic debris and other macrolitter in urban
runoff in a suburban catchment of Greater Paris. Water Res. 192, 116847.
https://doi.org/10.1016/j.watres.2021.116847

van Emmerik, T., Kieu-Le, T.-C., Loozen, M., Oeveren, K., Strady, E., Bui, X.-T., Egger, M.,
Gasperi, J., Lebreton, L., Nguyen, P.-D., Schwarz, A., Slat, B., Tassin, B., 2018. A
methodology to characterize riverine macroplastic emission into the ocean. Front.
Mar. Sci. 5. https://doi.org/10.3389/fmars.2018.00372

van Emmerik, T., Tramoy, R., van Calcar, C., Alligant, S., Treilles, R., Tassin, B., Gasperi, J.,
2019. Seine Plastic Debris Transport Tenfolded During Increased River Discharge.
Front. Mar. Sci. 6. https://doi.org/10.3389/fmars.2019.00642

524 Veerasingam, S., Mugilarasan, M., Venkatachalapathy, R., Vethamony, P., 2016. Influence
525   of 2015 flood on the distribution and occurrence of microplastic pellets along the
526   Chennai coast, India. Mar. Pollut. Bull. 109, 196–204.
527   https://doi.org/10.1016/j.marpolbul.2016.05.082
528 Vilmin, L., 2014. Modélisation du fonctionnement biogéochimique de la Seine de
529   l'agglomération parisienne à l'estuaire à différentes échelles temporelles (phdthesis).
530   Ecole Nationale Supérieure des Mines de Paris.
531 Voies Navigables de France, 2020. Transport et tourisme fluvial : les chiffres clés 2019.
532 Wagner, S., Klöckner, P., Stier, B., Römer, M., Seiwert, B., Reemtsma, T., Schmidt, C.,
533   2019. Relationship between Discharge and River Plastic Concentrations in a Rural
534   and an Urban Catchment. Environ. Sci. Technol. 53, 10082–10091.
535   https://doi.org/10.1021/acs.est.9b03048
536 Watkins, L., Sullivan, P.J., Walter, M.T., 2019. A case study investigating temporal factors
537   that influence microplastic concentration in streams under different treatment
538   regimes. Environ. Sci. Pollut. Res. Int. https://doi.org/10.1007/s11356-019-04663-8
539 Witzig, C.S., Földi, C., Wörle, K., Habermehl, P., Pittroff, M., Müller, Y.K., Lauschke, T.,
540   Fiener, P., Dierkes, G., Freier, K.P., Zumbülte, N., 2020. When Good Intentions Go
541   Bad—False Positive Microplastic Detection Caused by Disposable Gloves. Environ.
542   Sci. Technol. 54, 12164–12172. https://doi.org/10.1021/acs.est.0c03742
543 Wong, G., Löwemark, L., Kunz, A., 2020. Microplastic pollution of the Tamsui River and its
544   tributaries in northern Taiwan: Spatial heterogeneity and correlation with
545   precipitation. Environ. Pollut. 260, 113935.
546   https://doi.org/10.1016/j.envpol.2020.113935
547 Wu, P., Tang, Y., Dang, M., Wang, S., Jin, H., Liu, Y., Jing, H., Zheng, C., Yi, S., Cai, Z.,
548   2020. Spatial-temporal distribution of microplastics in surface water and sediments of
549   Maozhou River within Guangdong-Hong Kong-Macao Greater Bay Area. Sci. Total
550   Environ. 717, 135187. https://doi.org/10.1016/j.scitotenv.2019.135187
551 Zhao, S., Zhu, L., Li, D., 2016. Microscopic anthropogenic litter in terrestrial birds from
552   Shanghai, China: Not only plastics but also natural fibers. Sci. Total Environ. 550,
553   1110–1115. https://doi.org/10.1016/j.scitotenv.2016.01.112
554 Zheng, Y., Li, J., Sun, C., Cao, W., Wang, M., Jiang, F., Ju, P., 2021. Comparative study of
555   three sampling methods for microplastics analysis in seawater. Sci. Total Environ.
556   765, 144495. https://doi.org/10.1016/j.scitotenv.2020.144495
557

558 Supplementary data

559 Table S1: Daily flowrates, water levels and sampling volumes corresponding to each sample

560 (data from http://hydro.eaufrance.fr)

			Upstream	Downstream 1	Downstream 2
1	01/26/2018	Flowrates (m^3/s)	280	1570	1880
		Water level (m)	6.19	5.49	3.39
		Sampling volume (L)	23	27	19
2	02/05/2018	Flowrates (m^3/s)	330	1460	1940
		Water level (m)	6.28	5.28	5.03
		Sampling volume (L)	24	24	23
2bis	02/21/2018	Flowrates (m^3/s)	256	-	-
		Water level (m)	6.19	-	-
		Sampling volume (L)	24	-	-
3	07/17/2018	Flowrates (m^3/s)	45	155	241
		Water level (m)	4.01	0.97	3.36
		Sampling volume (L)	21	20	20

561

562 Table S2: Summary of microfibers and microplastics sizes collected during a flood event

Microfibers	N	Mean (µm)	Standard deviation (µm)	Median (µm)	Interquartile range (µm)
Upstream	164	4153	4388	2716	3092
Downstream 1	168	3762	3036	2670	2983
Downstream 2	123	3699	3254	2453	2863

563

Microplastics	N	Mean (µm)	Standard deviation (µm)	Median (µm)	Interquartile range (µm)
Upstream	158	278	351	171	185
Downstream 1	116	258	255	150	215
Downstream 2	80	243	201	163	198

564

565 Table S3: Summary of microfibers and microplastics sizes collected during low flow

566 conditions

Microfibers	N	Mean (µm)	Standard deviation (µm)	Median (µm)	Interquartile range (µm)
Upstream	51	3923	2705	3482	3536
Downstream 1	86	3363	2531	2512	2608
Downstream 2	122	3221	2337	2687	2675

567

Microplastics	N	Mean (µm)	Standard deviation (µm)	Median (µm)	Interquartile range (µm)
Upstream	45	133	116	96	90
Downstream 1	27	124	91	96	56
Downstream 2	75	386	409	249	390

568

569   Table S4: Details of the category "Other" from Figure 6

Polymers from the category "Other"	Abbreviation
Acrylonitrile butadiene styrene	ABS
Cellulose Acetate	CA
Polyacrylonitrile	PAN
Polyamide	PA
Polyurethane	PU
Polyvinyl Acetate	PVAC
Styrene butadiene rubber	SBR

570

571   Table S5 : Details of the polymers found in the different samples

	Number of polymer types found	Details
260118_Upstream	7	CA, PAN, PE, PES, PP, PS, PVC
260118_Downstream 1	5	ABS, PE, PP, PS, SBR
260118_Downstream 2	4	PE, PES, PP, PS
050218_Upstream	3	PE, PES, PP
050218_Downstream 1	5	PA, PE, PES, PP, PVAC
050218_Downstream 2	5	PA, PE, PES, PP, PU
210218_Upstream	6	PAN, PE, PES, PP, PS, PVAC
170718_Upstream	3	PE, PES, PP
170718_Downstream 1	5	PA, PE, PP, PS, PVC
170718_Downstream 2	5	ABS, PE, PP, PS, PVC

572

573

574   Table S6: MF and MP concentrations (first and third quartile) for each sampling site

	First and third quartile (concentration in microfibers per liter)	First and third quartile (concentration in microplastics per liter)	First and third quartile (concentration in µg of microplastics per liter)
Upstream	1.9-2.0	14.3-17.4	16.8-21.3
Downstream 1	3.0-3.4	12.3-15.6	3.9-10.3
Downstream 2	2.5-4.6	18.5-30.4	47.0-85.1

575